PROCEEDINGS OF SPIE

SPIEDigitalLibrary.org/conference-proceedings-of-spie

Overcoming pattern collapse of ultra high resolution dense lines obtained with EUV resists

A. Jouve, J. Simon, J. Foucher, T. David, J.-H. Tortai, et al.

A. Jouve, J. Simon, J. Foucher, T. David, J.-H. Tortai, Harun Solak, "Overcoming pattern collapse of ultra high resolution dense lines obtained with EUV resists," Proc. SPIE 5753, Advances in Resist Technology and Processing XXII, (4 May 2005); doi: 10.1117/12.598763

SPIE.

Event: Microlithography 2005, 2005, San Jose, California, United States

Downloaded From: https://www.spiedigitallibrary.org/conference-proceedings-of-spie on 08 May 2023 Terms of Use: https://www.spiedigitallibrary.org/terms-of-use

Overcoming Pattern Collapse of Ultra High Resolution Dense Lines Obtained with EUV Resists

A. Jouve, J. Simon, J. Foucher, T. David
CEA/DRT/LETI, 17 rue des martyrs, 38054 Grenoble cedex, France
Electronic mail: amandine.jouve@cea.fr

J-H Tortai
CNRS/LTM, 17 rue des martyrs, 38054 Grenoble cedex, France

H. Solak
Paul Sherrer Institute, LMN, 5232 Villigen, Suisse

ABSTRACT

Future lithography tools will have to address the 32 nm node. EUV lithography at 13.4 nm wavelength is the technology that may achieve such resolution if chemically amplified EUV resists show high enough resolution capabilities. However for sub 100 nm line width patterns, the pattern collapse, generated during the drying step of the developing process, becomes a serious limiting phenomenon.
We performed ultra high resolution exposures of EUV positive chemically amplified resists using either electron beam lithography (EBL), or EUV interferometry Lithography (IL) produced in a synchrotron. Two theoretical models have been compared with experimental results. One is mainly dealing with adhesion failure and the other with the line deformation. Adhesion failure occurs when capillarity pressure on the pattern become stronger than the attractive Van der Walls forces assuring the pattern adhesion on the substrate. Mechanical failure occurs once the lines deflection exceeds the mechanical breaking resistance of the resist. We highlighted that pattern collapse mode depends on resist thickness. Collapsing of patterns with thickness>100 nm are properly fitted with the deformation model of the resist; whereas for pattern height under 60 nm, experimental results obtained by EUVIL and EBL are properly predicted with the adhesion failure model.

To push resolution further and avoid pattern collapse, we targeted to expose sub 100 nm thick resist films. AFM3D measurements on EBL patterns show that reducing the resist thickness increases their top Line Width Roughness (LWR) testifying of physical resist properties variations in the resist interfacial layers. However we pointed out an optimum resist thickness, hence an optimal dilution. By tuning developer normality and puddle time, straight resist profiles were obtained. Finally we reached dense 40/40 nm lines in XP9947W150^{TM} resist using both exposure tools and validate the process compatibility with future etching steps by transferring 40/40 nm dense lines patterned with EBL into a metallic hard mask.

1. INTRODUCTION

Following the introduction of immersion lithography in microprocessor fabrication, EUV lithography at 13.4 nm is now planned to address the 32 nm node around 2013 [1]. To reach this goal, chemically amplified EUV resists must show very high resolution capabilities. Moreover, resist process development are necessary to be able to control acid diffusion in this length range [2]. Pushing present chemically amplified resists (CAR) to their resolution limit is the first step to tackle these issues. However, reaching critical resolution triggers additional processing problems, one of the first encountered being pattern collapse (PC) of small features printed in thick resist films.

Two solutions allow avoiding pattern collapse: decreasing the resist thickness or change the dry process step. Implementation of surfactants in the rinse step of the development [3] or in the developer itself [4] is the approach followed to avoid PC in production environment, especially in 193 nm lithography, where the minimum resist thickness is determined by etch resistance requirements. But for very small features, surfactants can not avoid pattern

Advances in Resist Technology and Processing XXII, edited by John L. Sturtevant,
Proceedings of SPIE Vol. 5753 (SPIE, Bellingham, WA, 2005)
0277-786X/05/$15 · doi: 10.1117/12.598763

Downloaded From: https://www.spiedigitallibrary.org/conference-proceedings-of-spie on 08 May 2023
Terms of Use: https://www.spiedigitallibrary.org/terms-of-use

collapse if the film is too thick. Ultra Thin Resist Films (UTRF) are needed for EUV resolution goals. Below a critical thickness (100 nm), the glass transition temperature of the resist is expected to vary within the resist depth due to air/resist and resist/substrate interfaces [5-6]. As the diffusion kinetic during the post exposure bake is strongly related to glassy transition; future lithography processes should be adapted to thin films.

In this study, we performed ultra high resolution exposures of EUV CARs of varying sensitivity, using either electron beam lithography (EBL), or EUV interferometry lithography (EUVIL). EBL has already shown 40/40 nm dense lines capabilities on electron beam resist [7] and EUVIL produced 26 nm length scale modulation in CAR [8]. Experimental details will be described in Part 2, and possibility to extrapolate EUVIL results based on EBL discussed Part 4.1. The origin of pattern collapse depending on resist thickness and exposure tool will be studied in part 4.2.Playing on resist dilution, we coated Ultra Thin Resist Films (UTRF) to avoid PC (Part 4.3). We reached dense 50/50 nm lines using both exposure tools. However resist profiles showed unacceptable features in term of integration, leading to further process optimisation. We finally achieved good printability: 40/40 nm dense lines with EUVIL and EBL, and checked integration by transferring the EBL pattern into a metallic hard mask (Part 4.4).

2. EXPERIMENTAL SET-UP

EUV exposures were conducted on the EUVIL beamline of the Swiss Light Source (SLS) at the Paul Scherrer Institute. This beamline is equipped with an undulator to generate photons with energy of 91 eV. Transmission membrane mask with gratings of varying period 2*p* were fabricated by patterning chromium on a Si_3N_4 membrane using EBL and reactive ion etching techniques [9-10]. EBL was performed on a LEICA VB6 UHR. Acceleration voltage is 100 kV, with beam size of 5 nm. Intensity used was 0.25 nA, with 10 nm Beam Step Size. Three EUVL photo resists EUV2D^{TM}, EUV12A^{TM}, and XP9947W150^{TM}, supplied by Rohm & Haas Microelectronics, coated on HMDS primed silicon substrates (either 200 mm diameter for EB exposures, or 100 mm for EUV exposures) were exposed. Resist films were Soft Baked (130°C/60s for EUV2D^{TM} and EUV12A^{TM}, 140°C/60s for XP9947W150^{TM}), Post Exposure Baked (130°C/90s), and developed using LDD26W. Patterned profiles were observed with SEM Hitachi 4000. Line Width Roughness (LWR) has been measured with AFM DimensionX3D from Veeco Instruments (AFM3D, noise level 2Å, Dynamic repetability 1 nm -3σ) equipped with a 64 nm diameter silicon flared tip. When AFM3D measurement is not feasible, Line Edge Roughness (LER) is measured using SUMMIT Software, provided by Patrick Naulleau of LBNL.

3. PATTERN COLLAPSE THEORY

Using EUVIL we were able to print 50 nm dense lines (1:1) into 140 nm thick EUV-2D resist as shown in Figure 3a. However, some lines suffered from pattern collapse (Figure 3b), indicating that no smaller Critical Dimension (CD) can be obtained with the same resist film thickness without undergoing PC.

Pattern collapse origin is related to the capillarity force generated from outside to inside the pattern during the evaporation of the rinse liquid after the developing process. The pattern collapses if the structures are not strong enough. Two mechanisms are possible to explain the pattern collapse: the “peeling” of the pattern or the ‘deformation’ of the structure. A design of experiment was carried out to evaluate the effect of rinse and dry rinse speed and acceleration values on pattern collapse. The only significant parameters are the resist thickness and the puddle time, as reported in literature [3, 17].

3.1 The capillarity force on patterns

During the rinse process, the rinse liquid remains between the pattern. The adhesion force of the liquid on the pattern is stronger than the surface tension of the rinse liquid which implies that the liquid surface is concave, as shown on figure 1.

Equation (1) shows the pressure from outside pattern to inside by the surface tension of the rinse liquid, where γ is the surface tension, and R the radius of curvature of the rinse liquid. This radius of curvature can also be described as in equation (2) where d is the distance between two patterns, h the resist height, D the pattern length and e the pattern CD. θ is the contact angle of the rinse liquid on the resist surface.

Lam Research Ex. 1012 - Page 3 Lam Research Corp. v. Inpria Corp. IPR2024-00033 - U.S. Patent No. 9,823,564

Downloaded From: https://www.spiedigitallibrary.org/conference-proceedings-of-spie on 08 May 2023
Terms of Use: https://www.spiedigitallibrary.org/terms-of-use

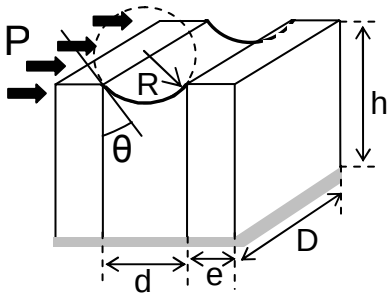

Figure 1: Schematic diagram of the capillarity force of the rinse liquid on two patterns after rinse process

$$P = \frac{\gamma}{R} \quad (1)$$

$$R = \frac{d}{2 \cdot \cos(\theta)} \quad (2)$$

Putting equation (2) into equation (1) results in the definition of the pressure of the rinse liquid on the pattern:

$$P = \frac{2 \cdot \gamma \cdot \cos(\theta)}{d} \quad (3)$$

3.2 Pattern degradation modes

3.2.1 Adhesion model

Pattern collapse attributed to the peeling mode is related to adhesion between resist and substrate. F. Tardif et al. expressed the breakdown threshold of "Posed" linear structure linked to the substrate by Van der Waals force (F_{vdw}) and submitted to capillarity force (F_{cap}) during rinse dry step, as equation (4) [11]:

$$\frac{F_{cap}}{\int_0^e x dF_{VdW}} = \frac{2 \cdot \gamma \cdot \cos(\theta) \cdot a}{A \cdot e \Big/ 6\pi \cdot a \cdot h_0^3} \quad (4)$$

Where h/e=a is the pattern aspect ratio, A the Hamaker constant, and h_0 the Lennard-Jones distance. PC occurs when the ratio equals or overrides 1. This equation is stated considering that no deformation of the pattern can be encountered, and the lines are simply deposited on the substrate.
For dense patterns (line=space), we deduce from equation (4) the critical aspect ratio a_c, value of the aspect ratio where pattern collapse is observed.

$$a_{c1} = \left[\frac{A \cdot h}{2 \cdot \gamma \cdot \cos(\theta) \cdot 6\pi \cdot h_0^3} \right]^{1/3} \quad (5)$$

3.2.2 Mechanical model

In the deformation mode case, the pattern break, bend, tear or lean against each other: this type of pattern collapse is related to the mechanical properties of the resist. Equations given by T. Tanaka et al. [19] and later supported by H.J Lee et al. [16, 18] model the bending of the pattern submitted to capillarity force linearly distributed on the height of the pattern (see figure 2). It expresses the balance between the surface tension force and the elastic force on the resist pattern.

In this model, the maximum deformation length δ on a pattern can be described as equation (6), where E is the Young modulus of the resist.

Lam Research Ex. 1012 - Page 4 Lam Research Corp. v. Inpria Corp. IPR2024-00033 - U.S. Patent No. 9,823,564

Downloaded From: https://www.spiedigitallibrary.org/conference-proceedings-of-spie on 08 May 2023
Terms of Use: https://www.spiedigitallibrary.org/terms-of-use

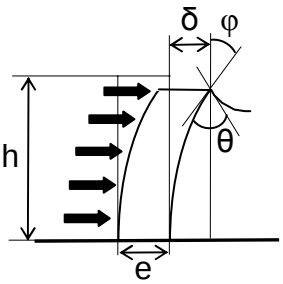

Figure 2: The distributed pressure on a pattern

$$\delta = \frac{w \cdot h^4}{8 \cdot E \cdot I} \quad (6)$$

I is the cross-sectional second moment of the pattern, and w the total pressure. They can be described trough equations (7) and (8) respectively.

$$I = D \cdot e^3 / 12 \quad (7) \qquad w = P \cdot D \quad (8)$$

Putting equations (7) and (8) into equation (6), results in equation (9) which described the deformation due to a distribution of pressure P:

$$\delta = \frac{3 \cdot P \cdot h^4}{2 \cdot E \cdot e^3} \quad (9)$$

The resulting critical aspect ratio calculated through this theory is:

$$a_{c2} = \left[\frac{E \cdot e^2}{24 \cdot h \cdot \gamma \cdot \cos(\theta)} \right]^{1/3} \quad (10)$$

These equations (6) to (10) come from the theory stated for a beam fixed by one of its extremity and submitted on all its right section to a uniform force density. A beam is defined as a solid in with one of its dimension is highly above the other one (minimal aspect ratio ≈ 8). In literature those equations has been validated on patterns obtained with 193 or 248 nm lithography (minimal pattern aspect ratios equals 7 eg: h=1 μm, e=0.075 μm). For lower aspect ratios, the solution of the stress tensor of the solid deformations could be different.

4. RESULTS AND DISCUSSION

4.1 EB Lithography as EUV Interference Lithography model

Similar resist profiles are observed in both type of exposures for original as well as diluted EUV2D™, EUV12A™, and XP9947W150™ resist. Moreover, sensitivity ratios of the three CAR tested remain the same between EUVIL and EBL. This may be explained as follows: 91 eV EUV photons are too energetic to directly generate Photo-Acid. PAG molecules are more probably degradated by electrons photo-emitted by excited resist atoms. This phenomenon is very similar to what is going on in EBL where the PAG decomposition is initiated by secondary electrons resulting from primary electrons collision. These observations supported our choice of carrying out tuning experiments with EBL, even though LER is considerably better: 3.4 ± 0.6 nm for EBL on 50 nm dense lines versus 10.1 ± 1.7 nm for EUVIL. Aerial image in the Gaussian EBL, particularly at 100 kV accelerating voltage, is by construction more contrasted than the sinusoidal IL aerial image. Lower aerial image contrast convoluted with CAR threshold behaviour triggers therefore higher LER.

4.2 Critical aspect ratio models for EUVIL and EBL

The aim of this set of experiments is to define the critical aspect ratio of positive chemically amplified resist under both EUVIL and EBL lithography. We expose the XP9947W150 original formulation and one dilution achieved by mixing 66% of resist with 33% of proper Added Solvent (AS). We obtain resist thicknesses ranging from 1400A down to 450A.
For all the thickness, we observe and characterize the 50/50 nm and 40/40 nm patterns by SEM top views and cross sections.

Lam Research Ex. 1012 - Page 5 Lam Research Corp. v. Inpria Corp. IPR2024-00033 - U.S. Patent No. 9,823,564

Downloaded From: https://www.spiedigitallibrary.org/conference-proceedings-of-spie on 08 May 2023
Terms of Use: https://www.spiedigitallibrary.org/terms-of-use

Figure 4 shows the experimental critical aspect ratios observed for both lithographies. Experimental a_c values for the 40/40 nm are difficult to obtain considering that for this resolutions the process window is extremely small.
Theoretical representation of the critical aspect ratios calculated from both theories: adhesion model (equation (5), grey curve) and mechanical model (equation (10), black curve) are also shown. The theoretical curves have been drawn with the set of parameters corresponding to polystyrene on SiO_2 surface in water [11] for the Hamaker constant ($A=10^{-20}$ J), h_0=0.4 nm, E=4e9 Pa, γ=0.072 N/m, θ=30° (contact angle of water on XP9947W150^{TM} resist measured experimentally).

First of all, according to the experimental results, 50/50 nm patterns can be properly printed into 160 nm resist film with EBL (a_c=3.13), and only 77 nm for EUVIL (a_c=1.7). For thicker films, the lines printed with EUVIL collapse as soon as they are partially opened. The CD of the pattern can't be measured; the data for thicknesses above 77 nm are thus not available with EUVIL.
One explanation of this difference could be supplied by the comparison of aerial images of EUVIL and EBL tools. Indeed it can be observed from figure 1b, that for high resist film thickness, EUVIL generates square profiles with a slight negative slope. Compared to vertical profiles, the radius of curvature of the rinse liquid between patterns is then increased, which implies higher values of the pressure at the top of the pattern (see equation (2) and (3)). However we have to keep in mind that the critical aspect ratio differences might also be related to slight process differences due to the use of different cleanrooms in EUVIL and EBL.

Secondly, it can be seen on figure 4 that the model which fit the best the experimental critical aspect ratios depends on the resist thickness.
On the one hand it can be seen that for thickness over 100 nm, the experimental EBL results are close to the model based on the mechanical properties described by equation (10).
For thin resist film, the experimental results observed with both EUVIL and EBL can be described with the model considering only the resist /substrate interaction (equation (5)).
In between these two thicknesses, we can observe a "transition" area, where pattern collapse phenomenon can't be properly described with one of these two models.

The good correlation between the experimental results obtain with EBL and the theory show that the mechanical equations stated for a beam can also describe the mechanical behaviour of resist pattern until a minimum aspect ratio value of 3,4 (h=96 nm).
For UTRF, the aspect ratio for 50/50 nm or 40/40 nm patterns is lower than 2, it is then coherent that the results obtained with EBL and EUVIL are not fitted by a mechanical model stated for beam.
For those dimensions, the elastic properties and the vertical deformation of the pattern can be then neglected comparing to its adhesion properties. Then for these dimensions, discussion should focus on pattern "lift-off". SEM observations for XP9947W150 show the limit thickness between partial lift off and collapse of the lines: it is found to be 60 nm (figure 5). For UTRF, pattern lift off can be described thanks to theories usually applied to molecular removal processes simulation (equation (4)). The low aspect ratios observed for the theoretical and experimental results for UTRF are due to the weak Van der Waals interactions of the resist with the substrate.

In between these two areas, the equations describing the pattern collapse phenomenon are complex. Indeed, both adhesion and mechanical forces have to be taken into account. This explains the experimental intermediate critical aspect ratios measured (see figure 4). A representative model is still under studies.

Through these results, we have shown that reducing the resist film thickness would not easily solve the problem of the pattern deformation during the development step of the lithographic process. Indeed, for thickness<60 nm the adhesion forces of the resist to the substrate rule pattern degradation, and leads to lower critical aspect ratio.
Further studies on resist chemistry formulation are still required to either increase the value of the Young modulus or the adhesion properties of the resist to the substrate without damaging the other resist properties (absorbance, deprotection speed reaction…). Those highly difficult studies can't be achieved in our laboratories.
To increase the critical aspect ratio of our pattern without undergoing chemistry studies, different surfactinated rinse solutions has been tested, but shown no significant improvements on EUV resists. Considering the low aspect ratio observed with EUVIL, we performed then optimization of several process parameters to improve resist profiles on low resist thickness films.

Lam Research Ex. 1012 - Page 6 Lam Research Corp. v. Inpria Corp. IPR2024-00033 - U.S. Patent No. 9,823,564

Downloaded From: https://www.spiedigitallibrary.org/conference-proceedings-of-spie on 08 May 2023
Terms of Use: https://www.spiedigitallibrary.org/terms-of-use

4.3 Ultra thin film study

4.3.1 Limits of resist dilution

Considering the viscosity of initial formulation of EUV resist, no sub 100 nm resist films can be obtained even with high spin coating speed. We performed dilutions of photo-resist in their respective solvent, for varying solvent fraction. For example, mixing 33% of EUV2D photo-resist with 66% of Added Solvent (AS), we were able to coat uniform 29.7 nm ± 1.3 nm thin films, and 44.7 nm ± 0.6 nm for 50 % AS dilution on 8 inch wafers.

In figure 5, SEM images of resulting resist profiles of EBL printed 50 nm dense lines are shown as a function of resist dilution, for resist EUV2D. Unacceptable top erosion of the resist as well as non-vertical slope were observed, characteristics which were not present in patterns printed in a thicker film (figure 3b).

As slope trend is usually explained in term of contrast lost, we performed DUV contrast curves as a function of resist dilution. Results are summarized in figure 7. Firstly, the dose to clear shifts with dilution and follows the resist swing curve as the film thickness decreases. Secondly, resist contrast γ_{PR} decreases from 5.2 to 0.17 $mJ.cm^{-2}.nm^{-1}$ for increasing dilution from 33 to 66% AS. In fact, no real threshold behaviour was visible for an AS fraction larger than 50%, which partly explains bad resist profiles observed. An eventual variation of chemical composition with dilution, due to increased affinity of some resist components with solvent, was checked using ATR Fourier Transform Infra-Red spectroscopy, and no visible difference arose with dilution. Nevertheless, stability of contrast between undiluted resist and 33% AS dilution enabled us to use low AS dilution.

4.3.2 Roughness of Ultra Thin Films

From the figure 6, it can be seen that resist profiles quality in term of integrability worsen with dilution (the thickness ranging from 130 to 30 nm): LER values measured with SUMMIT software increases from 3.4 ± 0.6 nm (left picture) to 22.3 ± 4.1 nm (right picture).

However, we can wonder which parameters between resist dilutions and resist thickness impact on the pattern degradation. To decorralate the impact of these two parameters, we exposed non diluted, and a 33% dilution (AS) of the XP9947W150 at varying thicknesses.

For rigorous analysis on we measured the Line Width Roughness (LWR 3σ) with the AFM3D when possible. The diameter of the silicon tip is 64 nm, which limits the measurements to 100nm dense lines printed with EBL.

Figure 8 shows the varying LWR versus thickness for varying pattern height and dilutions.
First, it can be observed on all the patterns a decrease of LWR through the pattern thickness. For example, on the XP9947W150 (h=135 nm) we measured LWR=26 nm for z=21 nm but LWR=9.7 nm when z=92 nm. If we compare all the pattern characterized, LWR results obtained are similar for all the pattern height at a given z value. Furthermore no obvious influence of resist dilution could have been shown.
Observing that, we can also add that the LWR on the top of the pattern increases when thinning the resist film. Those observations have been confirmed with LER measurements (SUMMIT software) on EUVIL patterns printed in XP9947W150. The figure 9 shows top views of EUVIL 50/50 nm dense lines printed into resist films varying from 90 nm to 25 nm.

The high roughness rate measured at the bottom of the patterns can partially explain the partial pattern lift off occurring observed in paragraph 4.2 on UTRF. Indeed, the Increasing roughness decrease the CD control, and generate smaller area in the line, which can be remove faster by the capillarity force because of their smaller adhesion surface to the substrate.

Secondly, it can be seen on figure 10 important rounding of the profile for 100/100 nm lines printed into XP9947W150 33% diluted for varying thickness from 98 nm to 55 nm. This increase of top erosion of the pattern can be related to Unexposed Film Thickness Lost (UFTL) measurements shown on figure 10.
Literature shows that Thin Resist Films can be described as a trilayer stack with differential physical and thermal properties [12-14]. One expression of these differential properties is confinement effects at the substrate/resist interface where molecular mobility is then reduced, whereas we observe higher mobility degree for the molecule of the air/surface interface. Results shown in figure 8 and 10 are coherent with those observations. Indeed the increasing

Lam Research Ex. 1012 - Page 7 Lam Research Corp. v. Inpria Corp. IPR2024-00033 - U.S. Patent No. 9,823,564

Downloaded From: https://www.spiedigitallibrary.org/conference-proceedings-of-spie on 08 May 2023
Terms of Use: https://www.spiedigitallibrary.org/terms-of-use

roughness at the resist/substrate interface and the erosion of the top of the pattern show a possible molecular gradient concentration of PAG or differential photogenerated acid diffusion through resist height.

U. Okoroanyanwu et al. observed an increase of air/resist surface layer thickness when total height of the pattern is under 50 nm [12]. Unfortunately sub 50 nm thick films can't be studied with AFM3D technology, and we didn't observed a thickness variation of interfacial Resist/Substrate layer. However ellipsometric measurements of Unexposed Film Thickness Loss (UFTL) as a function resist thickness (resist EUV2D) are presented in Figure 11. Values as large as 7 nm on 30 nm and 50 nm thick films were observed relatively far from printing area with a 0.26 normality developer which give evidence of a variation of polymer film structure for UTRF.

Finally, further tuning of the resist process for low added solvent fraction CAR (not over 33%) was done to ensure satisfactory resist profiles.

4.4 Developer dilution and puddle time optimization

With the optimized XP9947W150 dilution 33% coated at 3000 rpm (thickness = 80 nm), we targeted to obtain square profiles. In figure 11, additional UFTL measurements as a function of developer normality are reported. Decreasing developer normality up to 0.18 or 0.135 results in acceptable amount of dark erosion around 1 nm. By applying this less aggressive solutions on a 50% AS resist dilution, we are able to decrease LER from 12.4 ± 3.5 nm to 5.4 ± 0.9 nm and to improve considerably resist profiles as shown in SEM images of Figure 12, even if several drawbacks appeared as well. Reducing the developer normality results in increasing "T-top" profiles. Thus the radius of curvature of the rinse liquid increases; and considering the equation (1), the capillarity force increases and pattern collapse is promoted. Furthermore, the increased affinity between substrate and water leads to developer infiltration at the substrate/resist interface and increased pattern lift-off [15]. Reducing puddle time has the same consequences on the profiles than reducing developer normality. However we do observe profile improvements without relevant drawbacks for 20 s instead of 45s of puddle time.

We finally performed EUVIL and EBL exposures on diluted resists with 33% of AS and optimised developer normality and puddle time (N=0.18 for EUV12A and N=0.26 for EUV2D, N=0.26 for XP9947W150, puddle time=20s). We were able to print 40 nm dense lines without pattern collapse. The figure 13 sums up the optimization steps of the tuning process.

In order to validate the process compatibility with future etching steps, 40/40 nm dense lines patterned with EBL have been transferred into a metallic hard mask using chlorine based chemistry. No oxygen based ash process was performed in order to evaluate the resist selectivity versus metal etching as illustrated figure 14. The selectivity of the process was found to be 1,2.

5. CONCLUSION

By comparing experimental results to equation's models, we have shown that the mode of pattern collapse depends on the pattern height. For critical pattern aspect ratio above 3,4 only the mechanical properties of the resist have to be taken into account, and the pattern collapse can be fitted with equations stated for a beam deformation. In that case the pattern breaks or leans. For UTRF with resist thickness under 60 nm, the capillarity forces enhanced the pattern lift off because only the adhesion forces to the substrate have to be considered. As the Van der Waals interactions remain weak, the aspect ratios measured and simulated are low for UTRF (around 1,5 for the both exposure tools).

However, the use of thin resist film is the only relevant way of avoiding Pattern Collapse issues encountered when reaching smaller CD. We've shown the degradations encountered when using high resist dilution rates (resist contrast lost for AS rates higher than 33%). Top rounded resist profiles and increasing top-LWR when reducing the resist thickness have been measured with AFM3D on EBL patterns. They were attributed to physical resist properties variations in the interfacial layers combined with dark erosion during development.

Considering the XP9947W150 and other ESCAP resists supplied from Rohm and Haas material, we've shown that 40/40 nm dense lines with an aspect ratio of 1,7 could be obtained by EUV interference lithography using resist process optimised with Electron Beam Lithography.

Lam Research Ex. 1012 - Page 8 Lam Research Corp. v. Inpria Corp. IPR2024-00033 - U.S. Patent No. 9,823,564

Downloaded From: https://www.spiedigitallibrary.org/conference-proceedings-of-spie on 08 May 2023
Terms of Use: https://www.spiedigitallibrary.org/terms-of-use

ACKNOWLEDGMENTS: The authors would like to thank R. Brainard (Rohm & Haas Microelectronics, Marlboro, MA) for supplying samples and for fruitful discussions, P Käser for his participation in the EUVIL experiments and P. Naulleau of LBNL for providing the SUMMIT software.

REFERENCES

[1] International Technology Roadmap for Semiconductors 2003
[2] E. Lin et al., Science vol 297 (5580) p372
[3]*"Rinse liquid to improve Pattern Collapse"*, G. Lee et al., in Advances in Resist technology and processing XX, Proc. of SPIE, Vol. 5039 (2003) p 1416
[4]*"The Impact of surfactant in developer and rinse solutions on 193nm lithography performance",* P. Zhang et al., in Advances in Resist technology and processing XX, Proc. of SPIE, Vol. 5039 (2003) p 1409
[5] J.L Keddie et al., Europhysics letters, 27 (1) pp. 59-64 (1994)
[6] C.A Mack et al., J. Vac. Sci. Technol B 16 (6) pp. 3779-3783 (1998)
[7] S. Landis et al., Jap J of Applied Phys. to be published (2004)
[8] V. Golovnika et al., J. Vac. Sci. Technol B 22 (1) pp. 99-103 (2004)
[9] H.H Solak et al., Microelectronic Eng. 67-68 pp. 56-62 (2003)
[10] H.H Solak et al., J. Vac. Sci. Technol. B 20 (6) pp. 2844-2848 (2002)
[11]*" Mechanical resistance of fine microstructures related to particle cleaning mechanisms»,* F. Tardif et al., in PV ECS 2003-26, Cleaning Technology in Semiconductor Device Manufacturing VIII, Ed J. Ruzyllo et al.
[12] U. Okoroanyanwu, J. Vac. Sci. Technol. B 18 (6) pp 3381 (2000)
[13] " *Thin Film Confinement Effects on the Thermal Properties of Model Photoresists Polymers",* C. L. Soles et al., in J. Vac. Sci. Technol B 19 (6) pp 2690-2693.
[14] *"Glass Transition Temperature and Thermal Expansion Behaviour of Polymer Films Investigated by Variable Temperature Spectroscopic Ellipsometry"*, O. Kahle et al., in Thin Solid Films 313-314 (1998) 803-807
[15] *"Measurements of water distribution in thin lithographic films"*, B.D. Vogt et al., in Advances in Resist technology and processing XX, Proc. of SPIE, Vol. 5376 (2004), pp 56-62
[16]*"Resist Pattern Collapse modelling for Smaller Features"*, H.J. Lee et al., in J. Korean Phys. Soc., Vol. 42 (2003) pp S202-S206
[17] "*Improvement of Pattern Collapse issue by Additive Added DI water Rinse process"*, K. Tanaka et al., in Advances in Resist technology and processing XX, Proc. of SPIE, Vol. 5039 (2003) p 1366
[18] *"Resist Pattern Collapse with Top Rounding Resist Profile"*, H.J. Lee et al., Jpn. J. Appl. Phys. Vol. 42 (2003) pp.3922-3927
[19] "*Mechanism of Resist Pattern Collapse during Development Process"* , T. Tanaka et al., Jpn. J. Appl. Phys. Vol. 32 (1993) pp. 6059-6064

FIGURES

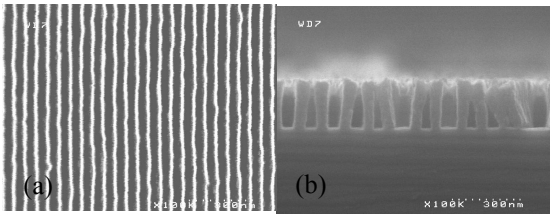

Figure 3: a. SEM Top View of 50 nm dense lines printed in resist EUV2D with EUV interferometry (left picture) b. Cross sections of some of these lines suffering from pattern collapse.

Downloaded From: https://www.spiedigitallibrary.org/conference-proceedings-of-spie on 08 May 2023
Terms of Use: https://www.spiedigitallibrary.org/terms-of-use

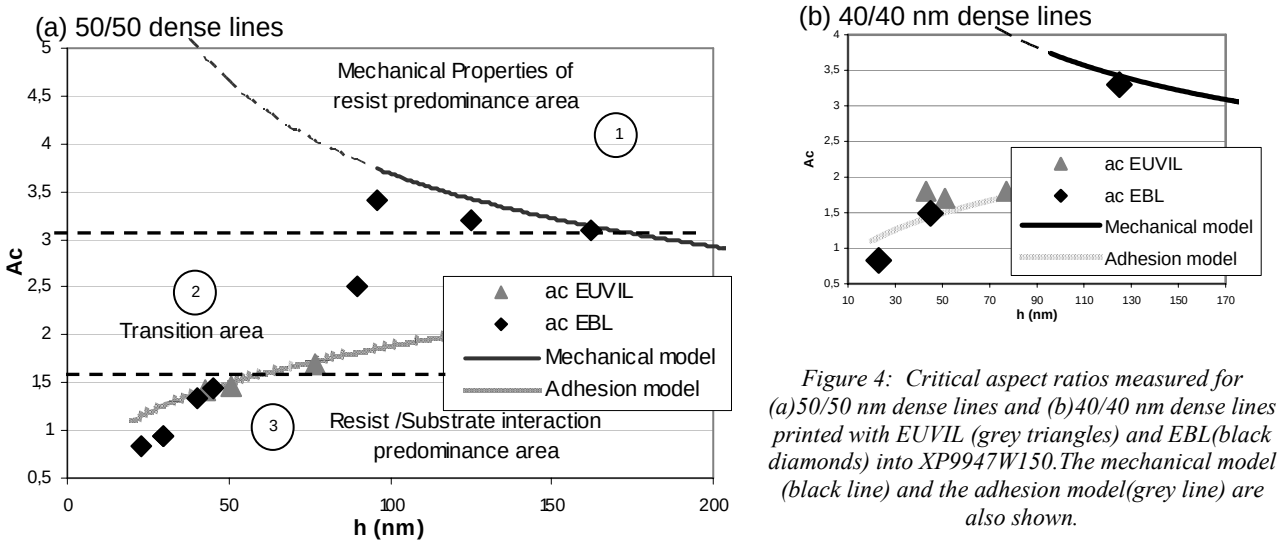

Figure 4: Critical aspect ratios measured for (a)50/50 nm dense lines and (b)40/40 nm dense lines printed with EUVIL (grey triangles) and EBL(black diamonds) into XP9947W150.The mechanical model (black line) and the adhesion model(grey line) are also shown.

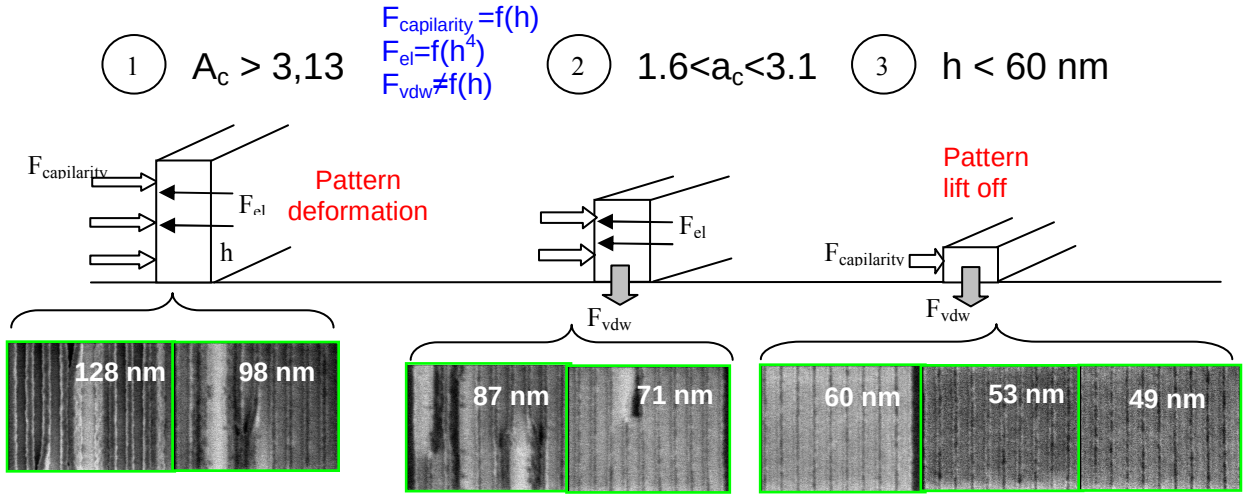

Figure 5: Representation of the different acting forces mode on a 50/50 nm EBL pattern for varying thickness of XP9947W150. 1/ Higher aspect ratio, mechanical model 2/Transition model where both adhesion and mechanical properties interfere.3/UTRF, adhesion properties of the resist to the substrate.

Downloaded From: https://www.spiedigitallibrary.org/conference-proceedings-of-spie on 08 May 2023
Terms of Use: https://www.spiedigitallibrary.org/terms-of-use

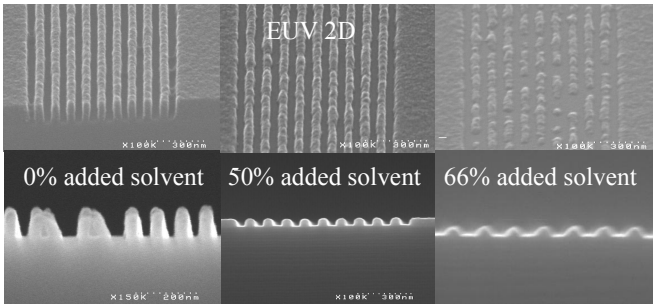

Figure 6: 50 nm Dense lines Top views and cross sections versus added fraction of solvent in resist EUV2D dilution (from left to right, no resist dilution, 50% AS, and dilution 66% AS)

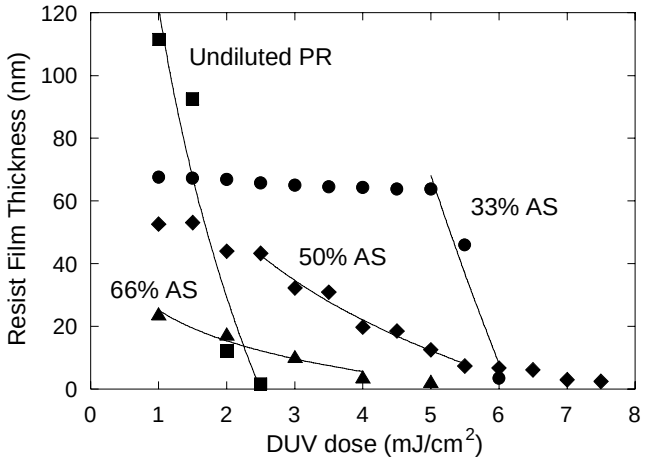

Figure 7: DUV Contrast curves for original EUV-12A resist (squares) and 3 dilutions: 33% AS (circles), 50% AS (diamonds), 66% AS (triangles).

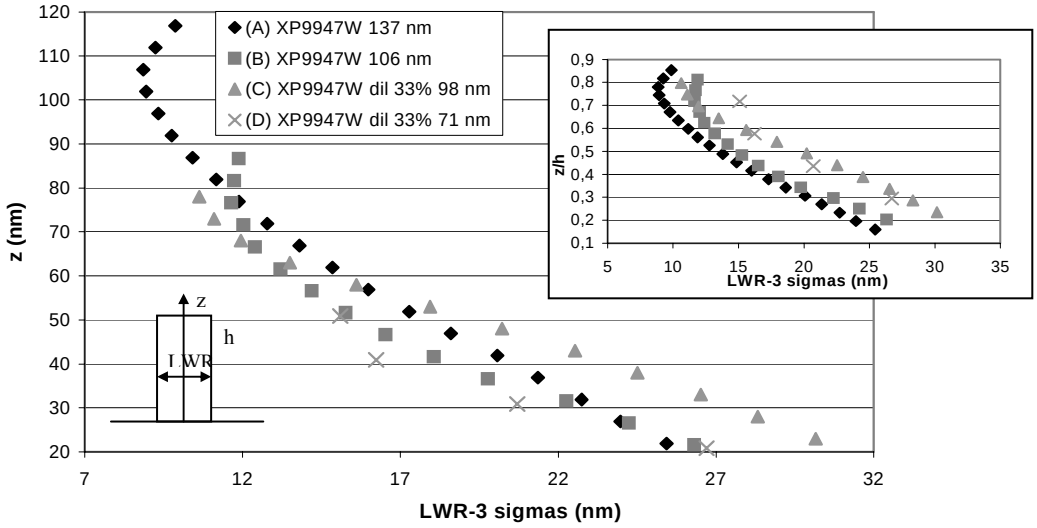

Figure 8: AFM3D measurements on 100/100 nm EBL patterns LWR(3σ) on Varying thickness and XP9947W150 33% AS.

Downloaded From: https://www.spiedigitallibrary.org/conference-proceedings-of-spie on 08 May 2023
Terms of Use: https://www.spiedigitallibrary.org/terms-of-use

T=250A	T=430 A	T=510 A	T=770 A	T= 900 A
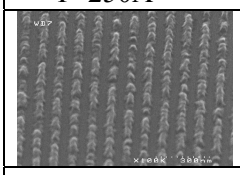	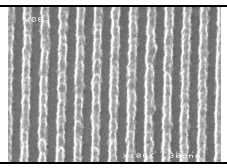	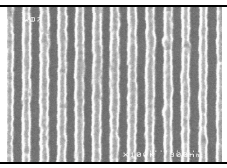	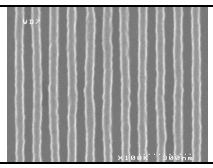	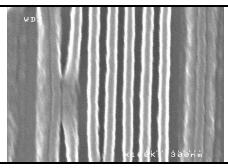
LER= 13 ± 1.8	LER=7.8 ± 2.2	LER=5.5 ± 1.1	LER=6.7 ± 1.7	LER=4 ± 0.8

Figure 9: EUVIL on XP9947W150 33% AS dilution: LER measurement with SUMMIT software on 50/50 nm pattern results for varying thickness and spin coating speed.

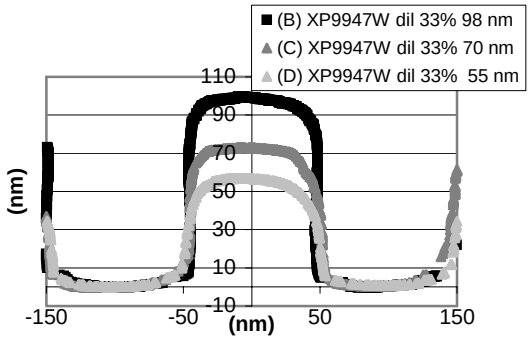

Figure 10: AFM3D profiles of 100/100 nm e-beam patterns into XP9947W150 33% AS diluted resist.

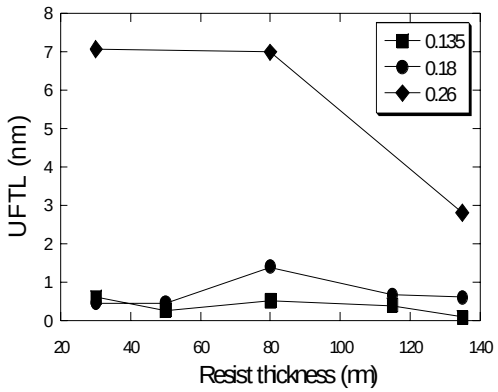

Figure 11: Unexposed Film Thickness Loss versus EUV2D resist thickness as a function of developer normality

Lam Research Ex. 1012 - Page 12 Lam Research Corp. v. Inpria Corp. IPR2024-00033 - U.S. Patent No. 9,823,564

Downloaded From: https://www.spiedigitallibrary.org/conference-proceedings-of-spie on 08 May 2023
Terms of Use: https://www.spiedigitallibrary.org/terms-of-use

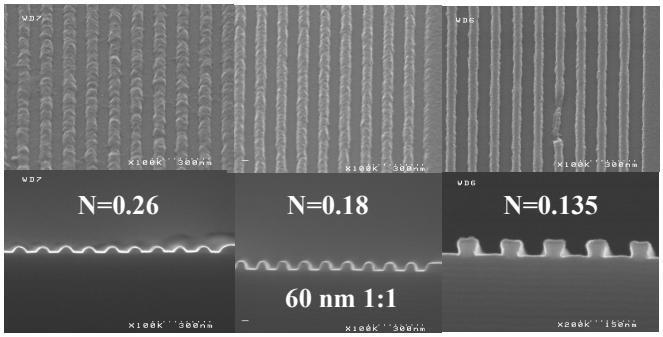

Figure 12: 60 nm Dense lines Top views and cross sections of EUV12A 50% AS diluted resist versus developer normality (from left to right, N=0.26, 0.18, and 0.135)

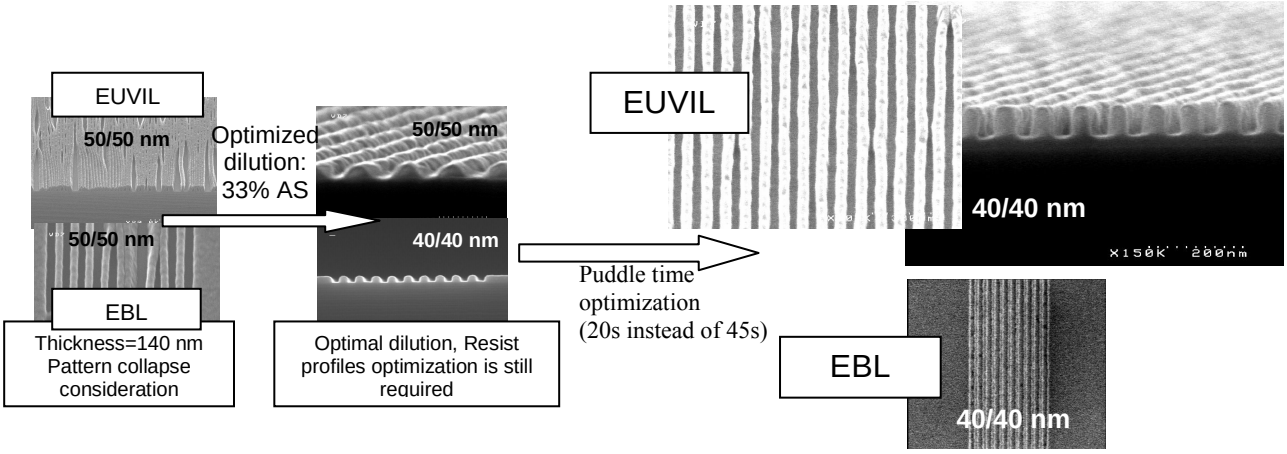

Figure 13: Process optimisation steps under EBL and EUVIL with the XP9947W150. 40/40 nm with good aspect ratio has been obtained on 77 nm thick films with the both technologies

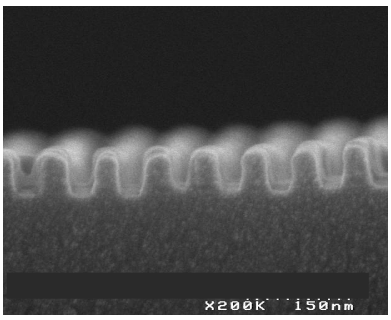

Figure 14: Etching transfer into a metallic hard mask of 40/40 nm lines patterned with EBL.

Lam Research Ex. 1012 - Page 13 Lam Research Corp. v. Inpria Corp. IPR2024-00033 - U.S. Patent No. 9,823,564

Downloaded From: https://www.spiedigitallibrary.org/conference-proceedings-of-spie on 08 May 2023
Terms of Use: https://www.spiedigitallibrary.org/terms-of-use